Published in final edited form as:
J Invest Dermatol. 2014 April ; 134(4): 1083–1090. doi:10.1038/jid.2013.479.

Melanocytes Are Selectively Vulnerable to UVA-mediated Bystander Oxidative Signaling

Robert W. Redmond[1], **Anpuchchelvi Rajadurai**[1], **Durga Udayakumar**[2], **Elena V. Sviderskaya**[3], and **Hensin Tsao**[1]

[1]Wellman Center for Photomedicine, Department of Dermatology, Massachusetts General Hospital, Boston, MA 02466

[2]Division of Molecular Radiation Biology, Department of Radiation Oncology, UT Southwestern Medical Center, Dallas, TX 75390-9038

[3]Cell Signalling Research Centre, Division of Biomedical Sciences, St. George's, University of London, London SW17 0RE, UK

Abstract

Long-wave ultraviolet A (UVA) is the major component of terrestrial UV radiation and is also the predominant constituent of indoor sunlamps, both of which have been shown to increase cutaneous melanoma risk. Using a 2-chamber model, we show that UVA-exposed target cells induce an intercellular oxidative signaling to non-irradiated bystander cells. This UVA-mediated bystander stress is observed between all three cutaneous cell types (i.e. keratinocytes, melanocytes and fibroblasts). Significantly, melanocytes appear to be more resistant to direct UVA effects compared to keratinocytes and fibroblasts although melanocytes are also more susceptible to bystander oxidative signaling. The extensive intercellular flux of oxidative species has not been previously appreciated and could possibly contribute to the observed cancer risk associated with prolonged UVA exposure.

INTRODUCTION

The cutaneous cellular community is chronically exposed to broad spectrum sunlight though most of the deleterious photochemical tissue interactions result from ultraviolet (UV) radiation. The impact of UV exposure on skin cancer production has been well established through many lines of study. Decades of epidemiologic research has unequivocally linked excessive sun exposure with an increased risk of developing both cutaneous melanoma and non-melanoma skin cancer (NMSC)(Almahroos and Kurban, 2004; Berwick and Halpern, 1997; Elwood and Jopson, 1997; Tsao and Sober, 1998). Perhaps the strongest direct evidence for UV participation in skin cancer formation comes from the high enrichment for C→T transitions at dipyrimidines sites in melanomas from solar-exposed locations compared to those from acral, sun-hidden regions(Alexandrov *et al.*, 2013; Berger *et al.*, 2012). Heritable defects in the repair of UV photoproducts results in xeroderma pigmentosum(Kraemer *et al.*, 1987; Lynch *et al.*, 1984)- a condition characterized by an excessive risk for melanoma among other skin cancers. Despite the substantial weight of evidence supporting the relationship between UV radiation and cutaneous carcinogenesis, the exact light-tissue interactions that govern this process are still not fully elucidated.

Correspondences: Hensin Tsao, MD PhD, Wellman Center for Photomedicine, Massachusetts General Hospital, Edwards 211, 48 Blossom Street, Boston, MA 02466. htsao@partners.org.

Conflict of Interest
The authors have no conflict of interest

A more recent line of evidence has emerged with the observed association between skin cancer risk and indoor sunlamps(Boniol *et al.*, 2012; Clough-Gorr *et al.*, 2008; Fears *et al.*, 2011; Han *et al.*, 2006). Most of energy from sunlamps is derived from long-wave UV radiation (i.e. UVA)(Autier *et al.*, 2011; Nilsen *et al.*, 2011). UVA has been shown to trigger a shower of short-lived reactive oxygen species(Noonan *et al.*, 2012; von Thaler *et al.*, 2010), which can generate 8-oxo-7,8-dihydro-2′-deoxyguanosine (8-oxo-dG)(Douki *et al.*, 2003) species and G→T transversions(Kozmin *et al.*, 2005). In animals, UVA has also been shown to harbor a direct melanomagenic effect (Noonan *et al.*, 2012). Unlike the fixed positional effects of direct DNA damage, UVA-induced ROS can freely diffuse and therefore theoretically cause near-neighbor bystander stress. Here we use a 2-chamber system to show that UVA induces a rich exchange of ROS between individual cell types resident in the cutaneous community. Our results show that melanocytes are selectively vulnerable to UVA-mediated bystander stress. Given the high keratinocyte-to-melanocyte ratio in normal skin, we suggest that UVA exposure initiates strong oxidative signaling that envelops cutaneous melanocytes, subjecting them to profound levels of oxidative stress.

RESULTS

In these studies, we selected primary human skin cells in order to avoid untoward effects of immortalization or transformation. Initial experiments determined direct effects of UVA on normal human melanocytes (NHMs), fibroblasts (NHFs) and keratinocytes (NHKs). Figure 1A shows dose-dependent toxicity for three skin cell types exposed to UVA under identical conditions of illumination and cell density. Among these cell types, pigmented NHMs appeared to be least susceptible to direct UVA toxicity. Figure 1B depicts the levels of oxidative stress (measured using the reactive oxygen species (ROS) probe, CMDHDCF) generated in each cell type as a function of UVA illumination (10 J/cm^2) with H_2O_2 as a positive oxidative control. Consonant with viability, melanocytes also generated lower amounts of ROS on direct UVA illumination although all three cell types were responsive to extracellular H_2O_2. This suggests that the presence of melanin may in fact protect against the effects of direct UVA exposure. To explore this possibility, we subjected immortalized C57BL6 melanocytes from normal (i.e. melan-a) and albino (i.e. melan-c2J) backgrounds to direct UVA irradiation (10 J/cm^2). Figure 1C shows that loss of melanin in the melan-c2J cells was associated with an increase in the level of ROS compared to the eumelanized melan-a cells. Taken together, these results reveal that human skin cells undergo oxidative stress upon UVA exposure and that pigmented melanocytes are more resistant to the direct effects of UVA compared to other skin cells. It also raises the possibility that intercellular flux of ROS between normal human cells may represent a previously unappreciated source of stress signaling.

To better characterize the collateral oxidative signaling induced by UVA irradiation, we created an interchangeable 2-compartment model (Figure 2A) to manipulate and to quantify bystander stress. As bystander effects are more pronounced at low fluence where damage occurs but cell killing is low(Chakraborty *et al.*, 2009), a fluence of 10 J/cm^2 UVA was chosen for all subsequent studies. In initial analyses, unirradiated melanocytes (i.e. bystander) that were co-cultured with either UVA-treated NHKs or NHFs (i.e. the targets) exhibited a consistent time-dependent increase in DCF fluorescence (Figure 2B). In contrast, bystander melanocytes co-cultured with unirradiated cells led to no appreciable induction of DCF fluorescence.

Experiments were then performed using all combinations of target and bystander populations to determine which cell types are receptive to bystander signaling and which cell types are efficient at generating signal when treated with UVA. Table 1 shows the corrected DCF fluorescence signal in the bystander wells after 90 minutes of co-culture with

UVA-illuminated target populations. As an ROS donor, keratinocytes appeared to generate the greatest amount of bystander stress upon UVA illumination. The greatest effect was in fact observed when keratinocytes and melanocytes were paired as target and bystander (corrected stress = 49.0 + 0.5), respectively. Similar results were obtained with two different sources of primary melanocytes. Overall, melanocytes had the highest mean "recipient" index compared to other cells (32.5 vs 11.3 and 14.3) suggesting that pigment cells experience the greatest bystander stress irrespective of which target cell type was treated with UVA. Interestingly, melanocytes were the least effective donors of stress signaling when irradiated as targets, consistent with the lower response upon direct UVA exposure (Figure 1). Keratinocytes appeared to be most resistant to bystander stress while fibroblasts showed intermediate efficiencies as both donor and recipient.

We next performed experiments to gain greater insight into the nature and extent of the signaling event. When the target fibroblasts were pre-treated with either extracellular catalase (a H_2O_2 scavenger) or diphenylene iodinium (DPI, an NADPH oxidase inhibitor), complete abrogation of DCF fluorescence in the melanocytes was observed (Figure 3A). These results document intercellular transmission of H_2O_2, and possibly other species, to bystander melanocytes upon UVA irradiation of co-cultured fibroblasts. In order to approximate the level of oxidative signaling, we generated a standard curve of DCF fluorescence based on amounts of direct H_2O_2 exposure (Figure 3B). Since the overall normalized melanocyte bystander DCF fluorescence (N=16 bystander determinations) was 23.02+9.3, it appears that bystander oxidative stress approaches approximately 40 μM peroxide-equivalents of ROS. Furthermore, as shown in Figure 3C, both direct UVA and bystander stress signaling caused DNA damage as measured by the comet assay.

Lastly, since p53 has been shown to mitigate ROS in melanocytes, we next determined if upregulation of p53 can attenuate the UVA-mediated bystander stress. In order to activate p53, we used the MDM2 antagonist nutlin-3, which is known to interrupt p53-MDM2 binding and to rescue p53 from proteasomal condemnation. As shown in, pretreatment of bystander melanocytes with nutlin-3, an MDM2 antagonist, increased cellular levels of p53 in NHMs. Strikingly, with induction of p53, there was a complete abrogation of bystander oxidative signaling in the melanocytes when co-cultured with UVA-targeted fibroblasts (Fig 4).

DISCUSSION

These studies make several important observations towards our understanding of UVA effects. A somewhat unexpected finding was that melanocytes were more resistant to direct UVA oxidative stress and the least efficient generator of bystander signaling while they were also paradoxically the most vulnerable recipients of bystander stress (Fig 5).

The level of oxidative stress experienced by melanocytes within the epidermis may thus be profound considering every melanocyte is embedded within a matrix of ~36 keratinocytes(Seiberg, 2001) and deeper fibroblasts. Using approximations from our system, we estimate that the amount of bystander stress experienced by melanocytes is roughly equivalent to 40 μM H_2O_2-equivalents. This is likely an underestimate since the 2-compartment model reflects oxidative flux diluted into a chamber filled with 500 μL of media. The cell-cell contiguity that actually exists in vivo would be significantly greater than the detectable amount in vitro. Furthermore, since human skin is stratified with keratinocytes resting on top of the melanocytes, the most active ROS "donors" are also the cells (i.e. keratinocytes) that come into primary contact with incoming UVA. Thus, one important biological implication of our findings is that a profound flux of near-neighbor ROS envelopes each melanocyte with every UVA exposure.

Our data suggest that stress from direct UVA exposure may be reduced in melanocytes because of melanin. There is a recent report that hypopigmented melanocytes from the *slaty* mouse (*Dct* mutation) exhibit heightened oxidative sensitivity to UVA irradiation(Wan *et al.*, 2009), which is consistent with our finding though our melan-c2J melanocytes are completely devoid of both eumelanin and pheomelanin due to a homozygous *Tyr* mutation(Bennett *et al.*, 1989). An earlier study also showed the UVA induced more membrane permeability and lipid peroxides in unpigmented melanocytes (i.e. melan-c) compared to pigmented ones (i.e. melan-a) and more ROS in fibroblasts compared to melanocytes(Kvam and Dahle, 2003). It should also be noted however that normal human melanocytes have been reported to maintain higher ROS levels compared to fibroblasts possibly due to its melanin content(Jenkins and Grossman, 2013). On the other hand, Wang et al. recently examined DNA photoproducts in the context of UVA irradiation and found that UVA exposure caused more oxidative DNA damage in human melanocytes compared to normal skin fibroblasts possibly due to melanin interference with DNA repair(Wang *et al.*, 2010). It should also be noted that the Wang study employed maximum UVA doses of 5-fold lower than used here for our study. Thus, the cells would have been subjected to a relatively low degree of insult where bystander effects contribute to a large degree. Even in a situation where all cells are irradiated, an “internal bystander” effect occurs where cell signaling amplifies the stress. We have previously shown this effect to be quite dramatic in the case of photosensitized oxidative stress(Rubio *et al.*, 2009) where the internal bystander effect is considerable in a 2D cell population. Thus, it is possible that melanin may have heterogeneous effects and may simultaneously absorb UVA photons and intracellular ROS while inhibiting DNA repair and enhancing oxidative DNA damage. Furthermore, innate differences between melanocytes and other cells independent of pigmentation may also exist. These interactions underscore the complex and unelucidated relationship between cell type, pigmentation, oxidative stress and DNA repair.

The nature of the oxidative signaling is still under investigation. Treatment of the intercellular content with catalase appears to fully abrogate the bystander effect thereby suggesting that H_2O_2 or an H_2O_2-like agent is the predominant signaling molecule. There is also evidence that p53 plays a role in attenuating UV-induced oxidative stress. Kadekaro et al. reported that combined UVA+UVB irradiation of primary human melanocytes is associated with a dramatic increase in oxidative DNA damage which can be mitigated by p53 that is induced by either alpha-melanocyte stimulating hormone or nutlin-3(Kadekaro *et al.*, 2012). Our results are consonant with these findings. Although ongoing studies are underway to characterize mechanistic details, p53 does appear to be an important homeostatic regulator of UVA-mediated stress at least in melanocytes.

There are several limitations to our studies. The flux of oxidative species between human epidermal cells in vivo may be different than the levels calculated in vitro in our 2-chamber model. The question of the likelihood of bystander effects being seen at distance in tissue was previously studied using ionizing radiation microbeam irradiation, where scattering is negligible and targeted and bystander cells are easily identified(Belyakov *et al.*, 2005; Sedelnikova *et al.*, 2007). Using this approach in total skin constructs it was clearly shown that DNA damage could be observed in bystander cells at distances of millimeters from the border of the targeted region. Thus, although the 2D system has its limitations, it is reasonable to expect the type of bystander responses observed to be recapitulated in tissue. An additional limitation is that melanosome transfer between melanocytes and keratinocytes in vivo may attenuate direct UVA exposure within the epidermis and thus mitigate bystander stress signaling. Both of these challenges will require more faithful 3-D organotypic systems and/or in vivo measurements, which are ongoing areas of investigation and technical development.

The public health implications cannot be understated. First, indoor sunlamps, which predominantly emit UVA, have been touted as "safe" given their relatively lower levels of genotoxic UVB(Autier *et al.*, 2011). Our studies employed a fluence of 10 J/cm^2 delivered at an irradiance of 10.5 mW/cm^2 for a duration of approximately 16 minutes. Literature reports of sunbed characteristics cite irradiances of ~20 mW/cm^2 UVA delivered to the skin for a fluence of 24–36 J/ cm^2 in a typical 20–30 minute session- a level higher than that delivered in our experiments(McGinley *et al.*, 1998). Additionally, the UVA irradiance at the earth's surface in several cities across the USA has been estimated to be around 2.5 mW/cm^2, hence, the fluence of 10 J/cm^2 is equivalent to just over an hour's exposure under physiological conditions(Grant and Slusser, 2005). Recent whole animal studies have also shown that UVA is fully competent to induce melanomas in a melanin-dependent manner and that UVA preferentially creates 8-oxo-dG, which results from ROS(Noonan *et al.*, 2012). Thus, our study broadens the scope of UVA-induced sun damage and perhaps speaks to the long-term effects of sunlamps. Furthermore, since sunlight itself is 90–98% UVA(Autier *et al.*, 2011), sunscreens that solely absorb UVB without significantly attenuating UVA will have little impact on the levels of diffusible ROS generated by keratinocytes upon solar UVA exposure.

In summary, the emerging connection between UVA and melanoma risk has uncovered fundamental gaps in our understanding of UVA photocarcinogenesis. Our findings suggest that near-neighbor cells within the cutaneous community are vulnerable to significant levels of bystander stress and that a dynamic flux of ROS may be created during intense whole-body UVA irradiation whether intentional from sunlamp use or unintentional from poor UVA sun protection.

MATERIALS AND METHODS

Cell culture and compounds

Primary neonatal human keratinocyes were a gift from Dr. James Reinwald at Brigham and Women's Hospital, Boston and were cultured in 75mL flasks with keratinocyte serum-free medium (KSFM; Invitrogen- Grand Island, New York) supplemented with bovine pituitary extract (final concentration of 25μg/ml), epidermal growth factor (EGF, final concentration of 0.2 ng/ml), 0.3mM $CaCl_2$ and 10% penicillin/streptomycin. Medium was exchanged every two days and keratinocytes were grown (passages 3–13) in the flask until 70% confluent. Human dermal fibroblasts (adult, HDFA) were purchased from Life Technologies™ (Grand Island, New York) and cultured in 10 cm diameter plates with Medium 106 (M-106-500; Life Technologies™) supplemented with low serum growth supplement (LSGS, 5 ml in 500 ml of media) (Life Technologies™) and 10% penicillin/ streptomycin. Medium was exchanged every 2–3 days and fibroblasts were grown in the plate until 90% confluent. Two sources of primary human epidermal melanocytes were used- adult, lightly pigmented (HEMa-LP) melanocytes were purchased from Life Technologies™ and neonatal foreskin melanocytes were obtained from Dr. Mark Pittelkow (Mayo Clinic, Rochester, MN). These melanocytes were cultured in 10 cm diameter plates in Medium 254 (Life Technologies™) containing human melanocyte growth supplement, (HMGS, 5 ml in 500 ml of media; Life Technologies™) and 10% penicillin/streptomycin. Medium was exchanged every 2–3 days and melanocytes were grown in the plate until 90% confluent. The primary human fibroblasts and keratinocytes used were less than passage 12. Primary human melanocytes with slightly different passages were used with similar results though no primary human melanocytes after passage 14 were used. Melan-a (nonagouti/ black (*a/a*), C57/BL6 background) and melan-c (albino ($Tyr^{c\text{-}2J}/Tyr^{c\text{-}2J}$), C57/BL6 background) cells were obtained through a collaboration with Dr. Elena V. Sviderskaya.

Twenty-four hours prior to experiment, media was removed and cells were trypsinized (0.25% Trypsin/EDTA) and replated in either 6 well plates (Becton-Dickinson, BD-353504) or companion transwell inserts (BD-353104). Wells were plated as 80,000 cells per well and inserts were plated at 40,000 cells per well. Treated cells in the inserts comprise the target population while untreated cells in the wells comprise the "bystander" population

Both diphenyleneiodonium chloride (DPI) and catalase were purchased from (Sigma; St. Louis, MO) and used at a final concentration of 1μM and 50 Units/ml, respectively.

UVA Treatment

Immediately prior to treatment the medium in the inserts was removed and replaced with 300 μl of HBSS. Inserts were irradiated from above with a UVP Blak-Ray UV lamp (Ted Pella, Inc, Reading CA) for a period of time sufficient to deliver a total fluence of 10 J/cm^2 to the sample. The typical irradiance was ~ 11 mW/cm^2, which required a total of about 15 min illumination. The spectral output of the lamp was measured using a calibrated SP-01 spectroradiometer (Luzchem, Ottawa, Canada). The output has a maximum wavelength around 365 nm and is entirely in the UVA spectrum with negligible UVB contribution.

Co-Culture—During UVA illumination of cells in the insert, the medium was removed from a partner well containing a non-illuminated cell population and replaced with 500 μl of HBSS (Life Technologies™). On completion of UVA-treatment the insert was placed in the companion well, designated as time zero. The insert has a semi-permeable membrane interface with 1 μm pore size that allows exchange of small molecules but cells are kept separate. Co-culture was then performed in a humidified incubator at 37°C with 5% CO_2. This is shown schematically in Fig. 2A.

Cell Viability—Viability was measured in cell populations by flow cytometry using either Biotium Viability/ Cytotoxicity Assay kit. Viability was also determined by confocal microscopy using the Live/Dead assay kit (cat number: MP-03224; Life Technologies™). Cells ~70–80% confluent were irradiated in a 35 mm plate, incubated for 4 hours and then removed by trypsinization, normalized in medium, washed in PBS and resuspended in Opti-MEM medium (Life Technologies™) for 30 minutes prior to insertion into a FACSCalibur Flow Cytometer (BD Biosciences, San Jose, CA). For confocal imaging, after irradiation, the cells were incubated for 4 hours in Opti-MEM medium and the Live/Dead Assay dyes were added and imaged.

Measurement of Oxidative Stress—Immediately following illumination of the insert a further 200 μl of HBSS containing 5-(and-6)-chloromethyl-2′,7′-dichlorodihydrofluorescein diacetate (CM-H_2DCFDA; Life Technologies™) was added to the insert to give a total volume of 500 μL in the insert with a final CM-H_2DCFDA concentration of 1.7 μM. At the same time the medium in the companion well was removed and replaced with 500 μL of HBSS containing CM-H_2DCFDA at a concentration of 1.7 μM. The insert was then placed in the companion well at time zero and placed in the incubator at 37°C. On oxidation, the non-fluorescent CM-H_2DCFDA is converted to the fluorescent product, 2′,7′-dichlorofluorescein (DCF).

At 15 minute durations the well plate was taken to the plate reader, the inserts removed and the fluorescence intensity in each well was measured using a SpectraMax M5 plate reader (Molecular Devices, Sunnyvale, CA) with excitation and detection at 488 nm and 525 nm, respectively.

Comet assay—The assay was performed using the Trevigen Comet Assay kit (Catalog #: 4250-050-K). 10μl of cell suspension (~10^5 cells) was added to 100 μl of low-melting point agarose and 100ml aliquot was then dropped onto a pre-coated slide. The slides were placed at 4°C in the dark for 10 minutes and then immersed in the pre-chilled lysis solution provided in the kit and incubated for 1 hour at 4°C. The excess buffer was drained and the slides immersed in freshly prepared alkaline unwinding solution (300mM NaOH, 1mM EDTA, pH =13) for 1 hour at room temperature in the dark. The slides were then placed in an electrophoresis tank, with pre-chilled alkaline electrophoresis solution (300mM NaOH, 1mM EDTA, pH >13 Electrophoresis was carried out for 20 minutes at 24 volts. The excess solution was drained and the slides were rinsed twice in deionized water for 5 minutes and then in 70% ethanol for 5 minutes. The slides were dried at <45°C for 10–15 minutes. 100 μl of diluted Syber gold (Stock 10,000X, Invitrogen: S-11494) was placed on the dried agarose and the slides were kept at 4°C for 5 minutes. Excess solution was removed and the slides were allowed to dry at room temperature. Slides were viewed using a confocal microscope (Olympus Fluoview FV1000, Ex /Em 495nm/537nm). For quantitative analysis 50 randomly chosen nuclei were considered and comet scoring performed using the Image J-comet assay plug-in.

Acknowledgments

This work was supported in part by a CDMRP grant (CA093588) from the U.S. Department of Defense and the generous philanthropic donors to the MGH Millennium Melanoma Fund. Mentorship and supervision for Dr. Durga Udayakumar was supported in part by a grant from the National Institutes of Health (K24 CA149202 to H.T.)

References

Alexandrov LB, Nik-Zainal S, Wedge DC, et al. Signatures of mutational processes in human cancer. Nature. 2013; 500:415–21. [PubMed: 23945592]

Almahroos M, Kurban AK. Ultraviolet carcinogenesis in nonmelanoma skin cancer part II: review and update on epidemiologic correlations. Skinmed. 2004; 3:132–9. [PubMed: 15133392]

Autier P, Dore JF, Eggermont AM, et al. Epidemiological evidence that UVA radiation is involved in the genesis of cutaneous melanoma. Curr Opin Oncol. 2011; 23:189–96. [PubMed: 21192263]

Belyakov OV, Mitchell SA, Parikh D, et al. Biological effects in unirradiated human tissue induced by radiation damage up to 1 mm away. Proc Natl Acad Sci U S A. 2005; 102:14203–8. [PubMed: 16162670]

Bennett DC, Cooper PJ, Dexter TJ, et al. Cloned mouse melanocyte lines carrying the germline mutations albino and brown: complementation in culture. Development. 1989; 105:379–85. [PubMed: 2806130]

Berger MF, Hodis E, Heffernan TP, et al. Melanoma genome sequencing reveals frequent PREX2 mutations. Nature. 2012; 485:502–6. [PubMed: 22622578]

Berwick M, Halpern A. Melanoma epidemiology. Curr Opin Oncol. 1997; 9:178–82. [PubMed: 9161798]

Boniol M, Autier P, Boyle P, et al. Cutaneous melanoma attributable to sunbed use: systematic review and meta-analysis. BMJ. 2012; 345:e4757. [PubMed: 22833605]

Chakraborty A, Held KD, Prise KM, et al. Bystander effects induced by diffusing mediators after photodynamic stress. Radiation research. 2009; 172:74–81. [PubMed: 19580509]

Clough-Gorr KM, Titus-Ernstoff L, Perry AE, et al. Exposure to sunlamps, tanning beds, and melanoma risk. Cancer Causes Control. 2008; 19:659–69. [PubMed: 18273687]

Douki T, Reynaud-Angelin A, Cadet J, et al. Bipyrimidine photoproducts rather than oxidative lesions are the main type of DNA damage involved in the genotoxic effect of solar UVA radiation. Biochemistry. 2003; 42:9221–6. [PubMed: 12885257]

Elwood JM, Jopson J. Melanoma and sun exposure: an overview of published studies. Int J Cancer. 1997; 73:198–203. [PubMed: 9335442]

Fears TR, Sagebiel RW, Halpern A, et al. Sunbeds and sunlamps: who used them and their risk for melanoma. Pigment Cell Melanoma Res. 2011; 24:574–81. [PubMed: 21362155]

Grant RH, Slusser JR. Estimation of ultraviolet-A irradiance from measurements of 368-nm spectral irradiance. J Atmospheric Oceanic Technol. 2005; 22:1853–63.

Han J, Colditz GA, Hunter DJ. Risk factors for skin cancers: a nested case-control study within the Nurses' Health Study. Int J Epidemiol. 2006; 35:1514–21. [PubMed: 16943234]

Jenkins NC, Grossman D. Role of melanin in melanocyte dysregulation of reactive oxygen species. Biomed Res Int. 2013; 2013:908797. [PubMed: 23555101]

Kadekaro AL, Chen J, Yang J, et al. Alpha-melanocyte-stimulating hormone suppresses oxidative stress through a p53-mediated signaling pathway in human melanocytes. Mol Cancer Res. 2012; 10:778–86. [PubMed: 22622028]

Kozmin S, Slezak G, Reynaud-Angelin A, et al. UVA radiation is highly mutagenic in cells that are unable to repair 7,8-dihydro-8-oxoguanine in Saccharomyces cerevisiae. Proc Natl Acad Sci U S A. 2005; 102:13538–43. [PubMed: 16157879]

Kraemer KH, Lee MM, Scotto J. Xeroderma pigmentosum. Cutaneous, ocular, and neurologic abnormalities in 830 published cases. Arch Dermatol. 1987; 123:241–50. [PubMed: 3545087]

Kvam E, Dahle J. Pigmented melanocytes are protected against ultraviolet-A-induced membrane damage. The Journal of investigative dermatology. 2003; 121:564–9. [PubMed: 12925216]

Lynch HT, Fusaro RM, Johnson JA. Xeroderma pigmentosum. Complementation group C and malignant melanoma. Arch Dermatol. 1984; 120:175–9. [PubMed: 6696469]

McGinley J, Martin CJ, MacKie RM. Sunbeds in current use in Scotland: a survey of their output and patterns of use. Br J Dermatol. 1998; 139:428–38. [PubMed: 9767287]

Nilsen LT, Aalerud TN, Hannevik M, et al. UVB and UVA irradiances from indoor tanning devices. Photochemical & photobiological sciences: Official journal of the European Photochemistry Association and the European Society for Photobiology. 2011; 10:1129–36. [PubMed: 21445424]

Noonan FP, Zaidi MR, Wolnicka-Glubisz A, et al. Melanoma induction by ultraviolet A but not ultraviolet B radiation requires melanin pigment. Nat Commun. 2012; 3:884. [PubMed: 22673911]

Rubio N, Fleury SP, Redmond RW. Spatial and temporal dynamics of in vitro photodynamic cell killing: extracellular hydrogen peroxide mediates neighbouring cell death. Photochemical & photobiological sciences: Official journal of the European Photochemistry Association and the European Society for Photobiology. 2009; 8:457–64. [PubMed: 19337658]

Sedelnikova OA, Nakamura A, Kovalchuk O, et al. DNA double-strand breaks form in bystander cells after microbeam irradiation of three-dimensional human tissue models. Cancer research. 2007; 67:4295–302. [PubMed: 17483342]

Seiberg M. Keratinocyte-melanocyte interactions during melanosome transfer. Pigment cell research / sponsored by the European Society for Pigment Cell Research and the International Pigment Cell Society. 2001; 14:236–42. [PubMed: 11549105]

Tsao H, Sober AJ. Ultraviolet radiation and malignant melanoma. Clinics in Dermatology. 1998; 16:67–73. [PubMed: 9472435]

von Thaler AK, Kamenisch Y, Berneburg M. The role of ultraviolet radiation in melanomagenesis. Exp Dermatol. 2010; 19:81–8. [PubMed: 20067521]

Wan J, Liu XM, Lei TC, et al. Effects of mutation in dopachrome tautomerase on melanosome maturation and anti-oxidative potential in cultured melanocytes. Zhonghua Yi Xue Za Zhi. 2009; 89:1707–10. [PubMed: 19957532]

Wang HT, Choi B, Tang MS. Melanocytes are deficient in repair of oxidative DNA damage and UV-induced photoproducts. Proc Natl Acad Sci U S A. 2010; 107:12180–5. [PubMed: 20566850]

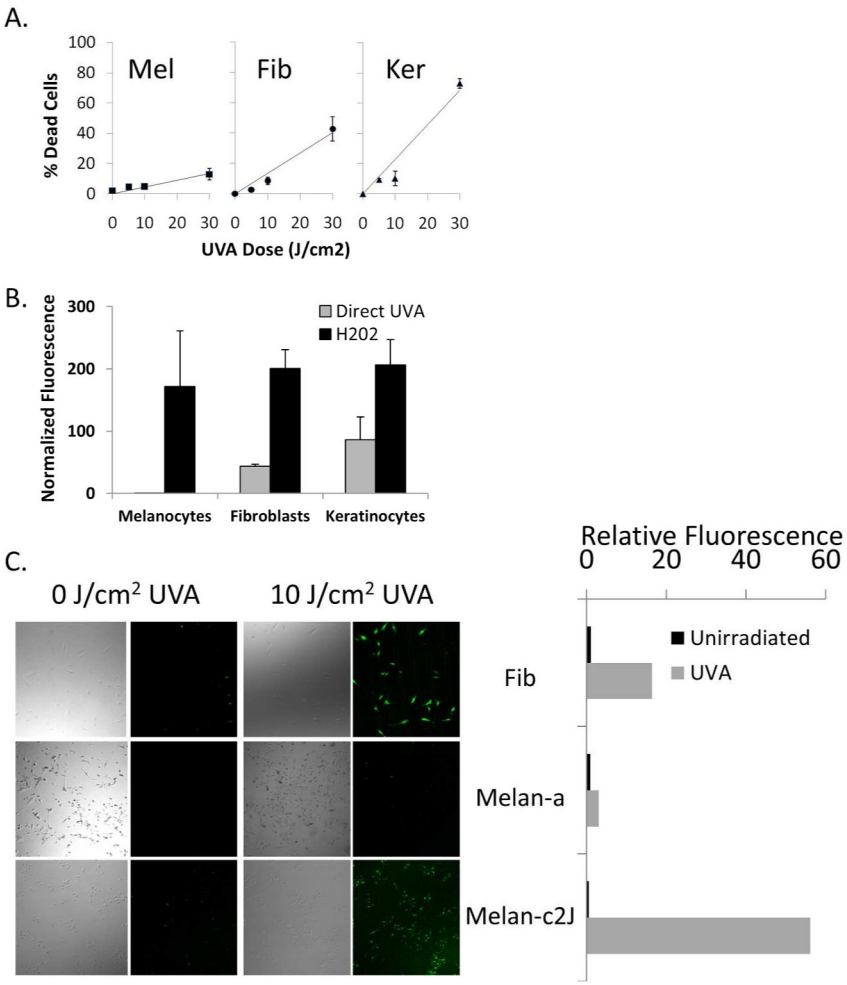

Figure 1. Direct oxidative and toxic effects of UVA on skin cells

(A) UVA induces less cytotoxicity in primary human melanocytes compared to fibroblasts or keratinocytes. Viability was determined by live/dead assay. **(B)** UVA (10 J/cm^2) elicits minimal 2′,7′-dichlorofluorescein (DCF) fluorescence in melanocytes compared to fibroblasts or keratinocytes while all 3 cell types respond similarly to H_2O_2 (200 μM). Error bars represent S.D. within a representative experiment; all experiments were repeated 2–4 times. **(C)** Immortalized murine melanocytes from nonagouti/black (*a/a)* mice on a C57/BL6 background (i.e. melan-a cells) and albino ($Tyr^{c\text{-}2J}/Tyr^{c\text{-}2J}$) mice on matched C57/BL6 mice (i.e. melan-c2J cells) were subjected to UVA (10 J/cm^2); primary human fibroblasts were used as a positive control. The level of DCF fluorescence was higher in the albino melanocytes and primary fibroblasts suggesting that the melanin in the eumelanized melan-a cells may have mitigated the intracellular ROS either directly (through ROS absorption) or indirectly (through UVA absorption) or both. In the bar graph, the amount of fluorescence was normalized to the amount of fluorescence observed in unirradiated fibroblasts (set as "1"). This experiment was repeated 3 times with similar results.

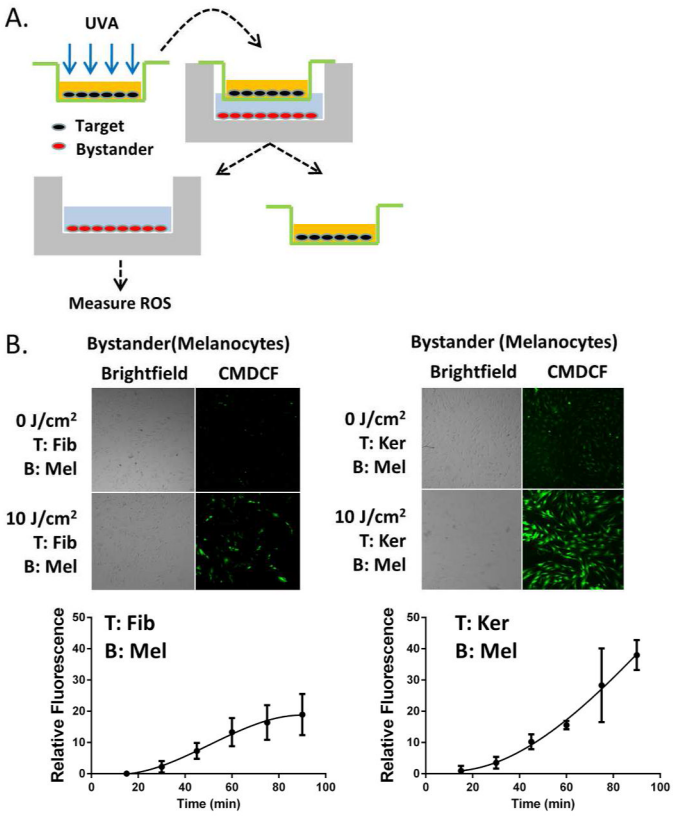

Figure 2. UVA-induced bystander effect

(A) 2-chamber (transwell/insert) model used to assess bystander stress. Wells were plated at 80,000 cells per well and inserts were plated at 40,000 cells per well. Treated cells in the inserts comprise the "target" population while untreated cells in the wells comprise the "bystander" population. **(B)** DCF fluorescence in unirradiated bystander melanocytes after 10 J/cm^2 UVA irradiation of target fibroblasts or keratinocytes. Upper panels show DCF fluorescence by imaging while lower panels show accumulation of *normalized* DCF fluorescence (DCF (10 J/cm^2) – DCF (0 J/cm^2)); thus, the graph illustrates time-dependent accumulation of UVA-mediated oxidative stress in bystander

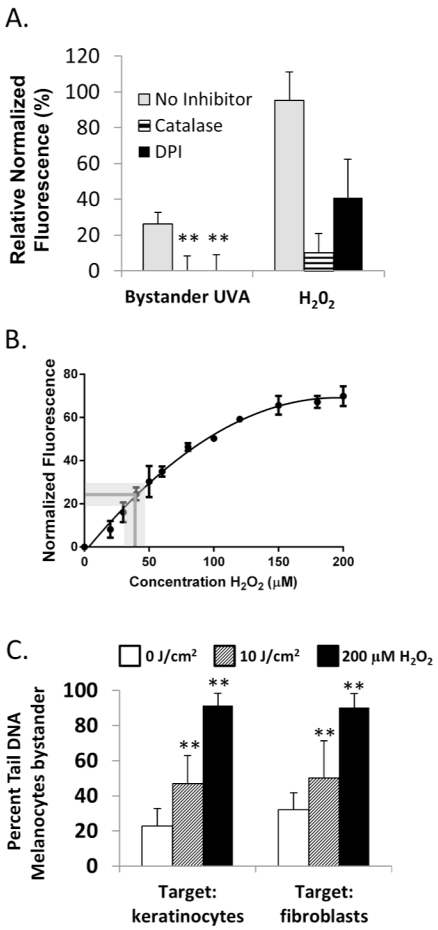

Figure 3. Characterization of intercellular signaling

(A) Loss of UVA bystander stress signaling after pre-treatment with either 50 U/mL catalase or 1 μM DPI. To compare across independent experiments, the normalized bystander DCF fluorescence was expressed a relative percentage of the H_2O_2 control fluorescence (relative normalized fluorescence). Error bars indicate average of 3 experiments. **(B)** H_2O_2 (varying concentrations indicated on x-axis) was directly added to primary human melanocytes and the DCF was measured at 90 min. This time point was chosen since the UVA bystander experiments were also performed at 90 min. In aggregate, the level of UVA-mediated bystander stress experienced by melanocytes lies within the gray region (N=16 independent bystander determinations), which corresponds to approximately the same amount of normalized fluorescence from exposure to 40 μM H_2O_2. **(C)** Significant increases in bystander melanocyte tail DNA after incubation of melanocytes with keratinocytes or fibroblasts which have been directly irradiated with UVA (100 J/cm^2) or directly exposed to H_2O_2 (200 μM). ** p<.001

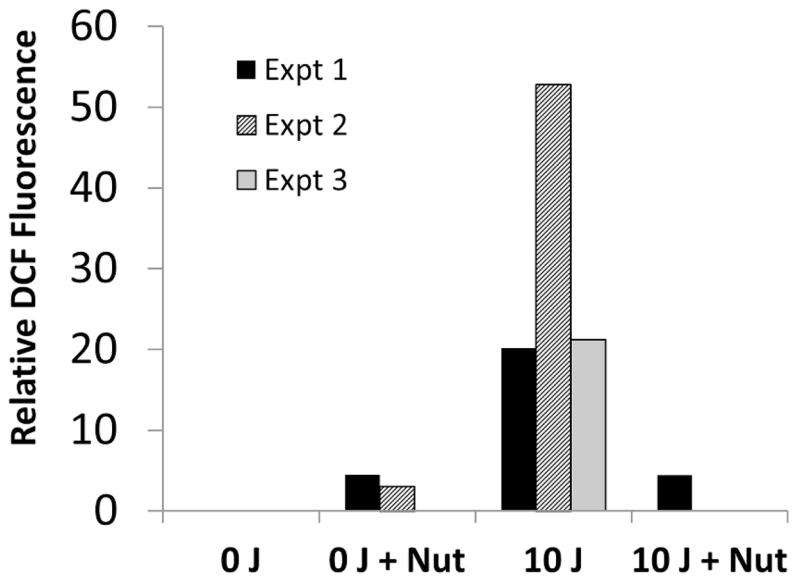

Figure 4. Induction of p53 protects against UVA-mediated bystander stress

Bystander primary human melanocytes were pre-treated with 5 μM nutlin-3 for 12 hours and co-incubated with UVA-irradiated target fibroblasts. The DCF fluorescence (relative to unirradiated, DMSO control at 90min reading) is shown. All 3 experiments demonstrated consistent induction of bystander stress, which was uniformly abrogated with nutlin-3 pre-treatment. Abbrev: Nut, nutlin-3.

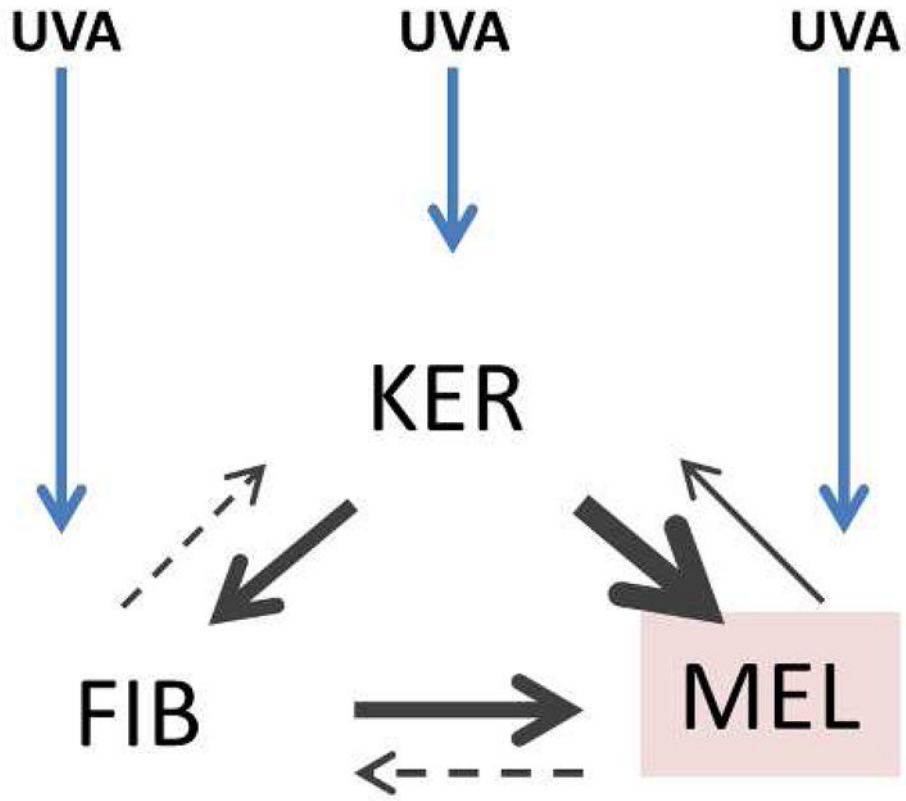

Figure 5. Bystander model in skin

Diagram illustrating level of bystander stress signaling between the three skin cell types (derived from Table 1). The thicknesses of the arrows correlate with level of stress induction. Keratinocytes communicate the most significant stress upon UVA exposure while melanocytes are relatively inefficient at signaling stress to other cell types. However, both fibroblasts and keratinocytes elicit substantial stress in melanocytes.

Table 1

Cell-cell UVA Bystander Stress Signaling

		UVA Target (ROS Donor)			
		Keratinocyte	**Melanocyte**	**Fibroblast**	***Mean "recipient" index*[‡]**
Bystander (ROS recipient)	**Keratinocyte**	20.4[#] ± 5.4 (3)[*]	13.5 ± 0.9 (4)	0 ± 6.4 (3)	*11.3*
	Melanocyte	49.0 ± 0.5 (8)	15.4 ± 3.5 (5)	29.5 ± 6.7 (4)	*31.3*
	Fibroblast	31.3 ± 1.4 (6)	0 ± 7.2 (4)	11.7 ± 4.7 (4)	*14.3*
	***Mean "donor" index*[†]**	*33.6*	*9.6*	*13.7*	

[#] To compare across experiments, we normalized UVA bystander stress to maximum observed with 200 μM H_2O_2 corrected stress = 100*(DCF_{10J}-DCF_{0J})/DCF_{H2O2}

[*] number of experiments shown in parentheses

[†] mean corrected stress among all recipients due to specific donor cell type (ie. average of column values)

[‡] mean corrected stress experienced by a single recipient cell type (ie. average of row values)